

# Aircraft Taxi Simulations with Detailed Aircraft and Landing Gear Modeling

Phillip W. Richards<sup>1</sup> and Boone M. Tate<sup>2</sup>  
*SDI Engineering Inc., Bellevue, WA, 98005, USA*

Isao Kuwayama,<sup>3</sup> Mitsuhiro Kurino,<sup>4</sup> and Hitoshi Isshiki<sup>5</sup>  
*Bridgestone Corporation, Kodaira-Shi, Tokyo, 188-8531, Japan*

December 5, 2022

This paper details the development and evaluation of a new aircraft taxi analysis method that can obtain a detailed steering, thrust, and braking profile for a given taxiing maneuver. The taxi maneuver in this case is defined as a path in the runway  $x, y$  plane and a velocity profile. Using a waypoint system, landing gear and subsystem design and analysis engineers can define the path and velocity profile and predict the thrust, steering and braking commands to the aircraft required for the aircraft to follow the path. When combined with a suitable aircraft and landing simulation capability, this algorithm can be utilized to provide a realistic simulation of the aircraft as it follows the prescribed path, capturing the important system nonlinearities, interactions, and subsystem response. SDI Engineering has applied this algorithm to GearSim, a proprietary landing gear and aircraft modeling and analysis software tool, for testing and evaluation of multiple aircraft models and taxi paths. Results from these test simulations indicate the algorithm is suitable for modeling and simulation purposes that can successfully predict the steering, thrust and braking inputs required for the taxi maneuver. Landing gear and subsystem design engineers can utilize these realistic simulations to understand the detailed loading conditions for their subsystems in routine taxi maneuvers. The developed algorithm could be also applied to improve autopilot systems for taxi maneuvers.

## I. Nomenclature

$\alpha_{NLG}, \alpha_{MLG}$	= nose and main landing gear slip angle
$\theta$	= nose landing gear steering angle
$\mu_x$	= main landing gear tire longitudinal friction coefficient
$\mu_{NLG}, \mu_{MLG}$	= nose and main landing gear tire lateral friction coefficient
$\mu_R$	= rolling coefficient of drag
$\sigma$	= relaxation length of tire
$\tau$	= time constant
$\psi$	= aircraft yaw angle
$\dot{\psi}$	= aircraft yaw rate
$a$	= aircraft forward acceleration
$A_1$	= first calibration factor to correct steering profile
$A_2$	= second calibration factor to correct steering profile
$A_{time}$	= time limit to change from $A_1$ and $A_2$
$B$	= braking factor to correct braking profile
$d$	= path segment length
$E$	= braking effort

---

<sup>1</sup> Principal Engineer, SDI Engineering Inc. AIAA Member.

<sup>2</sup> Mechanical Engineer, SDI Engineering Inc.

<sup>3</sup> Senior Technology Specialist, Bridgestone Corporation

<sup>4</sup> Solution Engineer, Bridgestone Corporation

<sup>5</sup> Solution Engineer, Bridgestone Corporation

$F_{Y,Tire}$	=	tire force in y-direction
$F_Z$	=	landing gear z-force
$F_{Brake}$	=	braking force
$g$	=	acceleration due to gravity
$I_{zz}$	=	yaw inertia
$K_x$	=	slope of longitudinal friction coefficient vs. slip ratio curve
$K_{NLG}, K_{MLG}$	=	nose landing gear, main landing gear cornering stiffness
$K^*$	=	ratio of main landing gear to nose landing gear cornering stiffnesses
$L_M$	=	longitudinal distance between center of gravity and main landing gear
$L_N$	=	longitudinal distance between center of gravity and nose landing gear
m	=	meters
MLG	=	main landing gear
$M_Z$	=	z-moment calculated about aircraft center of gravity
$M_{ZR}$	=	restoring moment from tires
$m_{AC}$	=	aircraft mass
$N_T$	=	number of tires per landing gear leg
NLG	=	nose landing gear
PID	=	proportional integral derivative
s	=	seconds
$s_m$	=	maximum slip ratio
$T$	=	total aircraft thrust
$t$	=	time for steering path determination
$V_i$	=	velocity at each path waypoint
$V_x$	=	aircraft forward velocity
$V_{X,Tire}$	=	component of tire velocity in tire x-direction
$V_{Y,Tire}$	=	component of tire velocity in tire y-direction
$x$	=	x-location of steering path waypoint
$y$	=	y-location of steering path waypoint

## II. Introduction

Aircraft landing gear and subsystems (e.g. tires, shock absorber, and structure) are typically designed considering extreme loading conditions, which may be experienced rarely by in-service aircraft. Detailed simulations of daily, lower-intensity aircraft maneuvers can provide a deep understanding of the typical loading conditions and enable fatigue, component wear predictions and subsystem performance. Aircraft taxi maneuvers are one example of these daily maneuvers, but can be challenging to model because the steering, thrust and braking commands required to follow an arbitrary path are not available. This paper details the development and evaluation of a new aircraft taxi analysis method that can obtain a detailed steering, thrust, and braking profile for a given taxiing maneuver. The taxi maneuver in this case is defined with a path in the runway  $x, y$  plane and a velocity profile. Using a waypoint system, users of this method can define the path and velocity profile. The developed taxi analysis then predicts the thrust, steering and braking commands to the aircraft required for the aircraft to follow the path. When combined with a detailed aircraft and landing gear analysis tool, the result is a realistic simulation of the aircraft as it follows the prescribed path, capturing the important system nonlinearities and interactions and subsystem response.

Methods for analyzing steering profiles in cars have been observed [1-3]. These methods typically involved analyzing the tire forces to predict how the vehicle would turn based on different inputs. Based on this method, a similar model was created and modified to account for typical aircraft geometry of two main landing gears (MLG) and one nose landing gear (NLG). This was done using a similar method as [4-6]; by using aircraft properties and geometry to analyze the tire forces during a turning maneuver. Steering analyses must also consider the tire relaxation length, which causes a delay in response as the forces build up in the tire [7, 8].

Aircraft landing gear consists of critical components that must be relied upon to function safely during the most challenging phases of flight. The landing gear consists of many coupled, nonlinear landing gear subsystems that can interact adversely to create dangerous conditions, including structural vibration, increased tire wear, and reduced braking system performance. SDI Engineering (SDI) has created GearSim, a proprietary landing gear and aircraft modeling and analysis software tool [9, 10] to analyze the load-carrying capability and dynamic response of these complicated structures. GearSim can simulate individual landing gear tests and whole aircraft cases, including

landing, takeoff, and ground maneuvering. However, even with a dedicated and powerful simulation software tool such as GearSim, one particular challenge with simulation of aircraft ground maneuvers is the need to include control commands from the pilot and automatic flight control, braking and steering systems to produce certain maneuvers. For takeoff and landing, this mainly consists of the thrust, flight control attitude commands and flap/spoiler deployment, and braking command profiles. For taxi maneuvers on aircraft runways, the pilot provides thrust, steering and braking commands to the aircraft to follow the desired path.

Development, testing and evaluation of the proposed steering prediction algorithm were performed by integrating the taxi analysis into GearSim. The majority of initial testing was performed on a narrow-body commercial aircraft model with a rigid landing gear model. The method has also been applied to some of SDI’s other aircraft models including generic wide-body aircraft models, and those including airframe and landing gear flexibilities.

### III. Steering, Thrust, and Braking Prediction

#### A. Modeling and Simulation Environment

GearSim’s holistic approach to the aircraft and landing gear modeling [9, 10] captures the important nonlinearities and creates a realistic simulation. This enables engineers focused on the individual subsystems such as tires, brakes, and hydraulic system component manufacturers to understand the realistic loading environment, and accurately predict the performance. GearSim’s modular simulation environment enables replacement of individual subsystems with user-created “black-box” models that can enable accurate modeling of proprietary subsystems without sharing the source code with SDI. GearSim is also an ideal platform to study novel landing gear concepts or complicated landing maneuvers; for example, aft wheel steering, off-runway operations, and carrier landings [10] are topics that have been studied using GearSim.

GearSim contains library examples that include generic Narrow-Body Commercial (NBC), Wide-Body Commercial (WBC), and Wide-Body Commercial 6-Wheel (WBC6) aircraft. These aircraft models were used to provide mass, inertia, landing gear geometry, and tire properties for use in the sample calculations shown below. The models were also used in full-fidelity simulations, applying the predicted steering, thrust and braking inputs developed by the taxi analysis.

#### B. Path and Steering Determination

The first step in analyzing a taxi maneuver is to define a path for the aircraft to follow by defining a list of waypoints. To model taxi maneuvers on different airports, the taxi waypoints can be chosen from the runway layout or from GPS data from instrumented aircraft. These are then interpolated linearly, with each corner point being joined by a tangent arc to maintain more feasible, smooth turns. The simple turn shown in Fig. 1 was created using four waypoints.

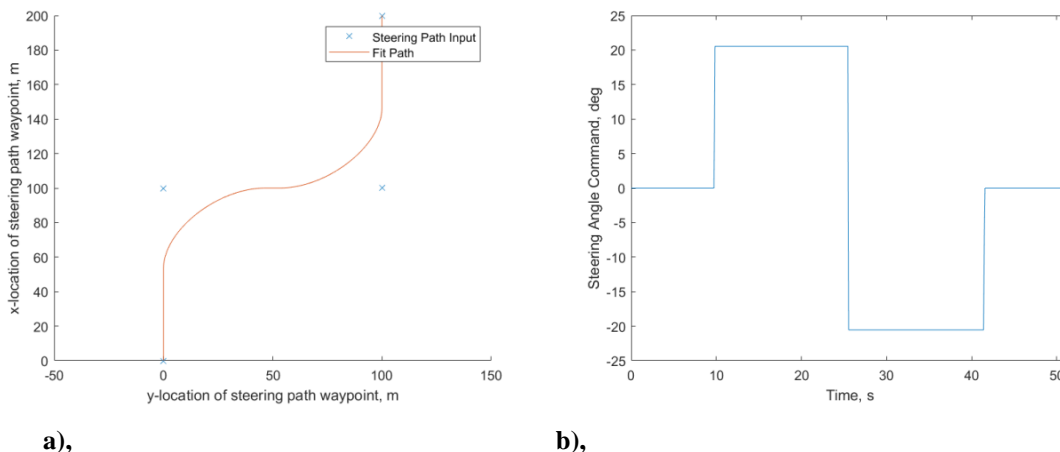


Fig. 1 Example Steering Path Input (a) and Steering Angle Command (b).

Using the smoothed path, the desired yaw angle of the aircraft at every point along the path is determined from Eq. (1). The velocity is interpolated along the path either linearly or with a constant acceleration method. Although a linear velocity interpolation is the simplest approach, it results in a varying acceleration profile. To obtain a constant acceleration profile, the path is subdivided into sections based on the user waypoint definitions and the acceleration is calculated for each section. For each segment along the path for a given section,  $V_i$  is updated according to constant acceleration  $a$  using the segment length  $d$ .

$$\psi = \tan^{-1} \left( \frac{y_{n+1} - y_n}{x_{n+1} - x_n} \right) \quad (1)$$

$$V_{i+1} = \sqrt{V_i^2 + 2ad} \quad (2)$$

The required yaw rate along the path is found from taking the derivative of the yaw angle vs. time relation.

$$\dot{\psi} = \frac{\psi_{n+1} - \psi_n}{t_{n+1} - t_n} \quad (3)$$

Given the required yaw rates for the maneuver, a relation between yaw rate and steering angle was needed to determine the steering angle along the path. Figure 2 shows diagrams of the aircraft and tire coordinate systems with the relevant steering forces labeled. On the left, a diagram of the three landing gears is shown with the forces acting on each tire. On the right, a diagram of the tire shows the model for lateral force as a function of the tire slip angle. Note for this diagram, the restoring moment due to offset of  $F_{y,Tire}$  is neglected for the purposes of this discussion, but will be mentioned later.

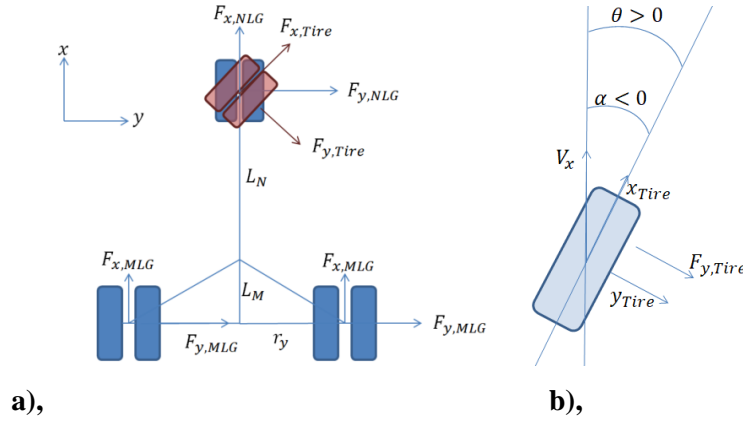


**Fig. 2 Summary of Aircraft Forces (a) and Tire Forces (b).**

Considering the NLG tire, the velocity of the tire in the aircraft frame is found by rotating the velocity at the NLG, which is composed of the forward velocity and a rotation component.

$$V_{Tire,NLG} = \begin{bmatrix} \cos(\theta) & \sin(\theta) \\ -\sin(\theta) & \cos(\theta) \end{bmatrix} \begin{Bmatrix} V_x \\ L_N \dot{\psi} \end{Bmatrix} \quad (4)$$

The slip angle of the nose and main landing gear tires can be linearized for small steering angles. For small slip angles, a linear stiffness can be applied to find the lateral friction coefficient. The lateral friction coefficient is multiplied by the tire force to generate a lateral force in the tire's y-direction. For small steering angles, this can be assumed to be equal to the force in the aircraft's y-direction.

$$\alpha_{NLG} = \frac{V_{Y,Tire}}{V_{X,Tire}} = \frac{-\sin(\theta) V_x + \cos(\theta) * L_N * \dot{\psi}}{\cos(\theta) V_x + \sin(\theta) * L_N * \dot{\psi}} \cong -\frac{V_x \theta - L_N * \dot{\psi}}{V_x} \quad (5)$$

$$\alpha_{MLG} = \frac{-L_M \dot{\psi}}{V_x - r_{yMLG} \dot{\psi}} \cong -\frac{L_M * \dot{\psi}}{V_x} \quad (6)$$

$$F_{Y,Tire} = F_Z \mu_{NLG} = -F_Z K_{NLG} \alpha_{NLG} \cong F_{Y,NLG} \quad (7)$$

A simplified estimate of the yawing moment, neglecting the restoring moment of the tires, is given by multiplication of the normal force on the nose and main landing gears by the lateral friction coefficient and x-distance to the center of rotation. The restoring moment on the tire is due to a shift of the tire force by the pneumatic trail, therefore to include the effect of restoring moment is to adjust the values of  $L_N$  and  $L_M$  in the following equation. Note the pneumatic trail is small compared to  $L_N$  and  $L_M$ , which makes the following approximation reasonable.

$$M_Z = M_{z,NLG} + 2M_{z,MLG} + M_{ZR} \cong \mu_{NLG} F_{z,NLG} L_N - 2\mu_{MLG} F_{z,MLG} L_M \quad (8)$$

$$F_{z,MLG} = \frac{m_{AC} * g}{2(1 + L_M/L_N)} \quad (9)$$

$$F_{z,NLG} = 2 * F_{z,MLG} * \frac{L_M}{L_N} \quad (10)$$

The above equations can be combined to form a linearized equation for yawing moment as a function of steering angle and yaw rate, which can then be set equal to  $I_{zz} \ddot{\psi}$ .

$$M_Z \cong F_{z,NLG} L_N K_{NLG} \frac{V_x \theta - L_N * \dot{\psi}}{V_x} - 2F_{z,MLG} L_M K_{MLG} \frac{L_M * \dot{\psi}}{V_x} \quad (11)$$

$$M_Z \cong L_M \frac{ACMASS * g}{\left(1 + \frac{L_M}{L_N}\right)} \left( K_{NLG} \frac{V_x \theta - L_N * \dot{\psi}}{V_x} - K_{MLG} \frac{L_M * \dot{\psi}}{V_x} \right) = C_1 \theta - C_2 \dot{\psi} = I_{zz} \ddot{\psi} \quad (12)$$

$$C_1 = L_M 2F_{z,MLG} K_{NLG} \quad (13)$$

$$C_2 = L_M 2F_{z,MLG} (K_{NLG} L_N + K_{MLG} L_M) / V_x \quad (14)$$

This equation can be rearranged to the classical first order lag equation to determine the time constant:

$$\frac{I_{zz}}{C_2} \ddot{\psi} + \dot{\psi} = \frac{C_1}{C_2} \theta \quad (15)$$

$$\tau = \frac{I_{zz}}{C_2} = \frac{I_{zz} V_x}{2F_{z,MLG} L_M (K_{NLG} L_N + K_{MLG} L_M)} \quad (16)$$

The above is useful to calculate the time delay due to aircraft inertia for potential use in the steering angle prediction algorithm. To find a closed-form solution for the steady-state, set  $M_z$  to zero (i.e. zero yaw acceleration in Eq. (12)) and solve:

$$\left( K_{NLG} \frac{V_x \theta - L_N * \dot{\psi}}{V_x} - K_{MLG} \frac{L_M * \dot{\psi}}{V_x} \right) = 0 \quad (17)$$

$$\theta = \frac{\left( L_N + L_M \frac{K_{MLG}}{K_{NLG}} \right) \dot{\psi}}{V_x} = \frac{(L_N + L_M K^*) \dot{\psi}}{V_x} \quad (18)$$

From these equations, as well as initial studies using GearSim, a linear relation was observed at steering angles from 0 to ~20 degrees, allowing for the use of a simplified linear model in most steering cases. This model was based on  $V_x$ ,  $\dot{\psi}$ , the longitudinal placement of the MLG and NLG, the ratio of tire cornering stiffnesses, and additional factors  $A_1$  and  $A_2$  to correct for any discrepancies between the predicted path and simulated results. For tuning purposes, the calibration factor can be separated into two or more segments, for example:

$$\theta = \begin{cases} \frac{A_1}{V_x} (L_N + L_M K^*) \dot{\psi} & t < A_{time} \\ \frac{A_2}{V_x} (L_N + L_M K^*) \dot{\psi} & t \geq A_{time} \end{cases} \quad (19)$$

To verify the conclusions from the path and steering equations presented above, a MATLAB script was developed. The linearizations made in the equations above were not made here, and instead a set of geometrically exact relations were used to account for the steering angle and the tire slip angles. For the relationship between tire lateral friction coefficient and tire slip angle, the linear method above in Eq. (7) was programmed, as well as a nonlinear table lookup between steering angle and lateral friction as shown below in Fig. 3.

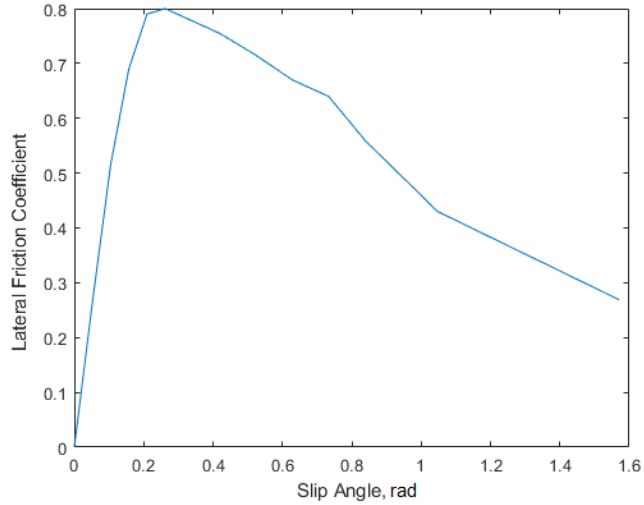


**Fig. 3 Nonlinear Lateral Friction Coefficient with Slip Angle Model.**

The MATLAB script was set up to solve for the steady-state yaw rate by using a Newton-Rhapson iteration for a given steering angle, varying the yaw rate until the yaw acceleration was zero. The resulting relation between steering angle and yaw rate for a linear tire model, nonlinear tire model, and simplified linear model, varying velocities and aircraft types, is shown in Fig. 4, with forward velocities provided in units of m/s. The aircraft types are GearSim's Narrow-Body Commercial (NBC), Wide-Body Commercial (WBC), and Wide-Body Commercial 6-Wheel (WBC6) models, which are representative of three different aircraft sizes. These show a linear response of the yaw rate with increasing steering angle within 0 and 20 degrees, with the corresponding values of  $A$  shown, selected through a linear fit between 0 and 20 degrees steering angle.

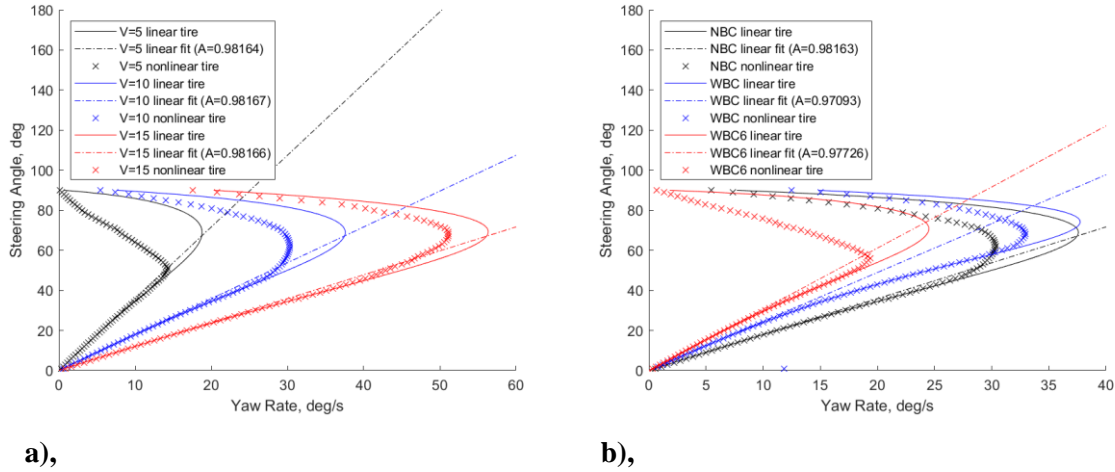


**Fig. 4 Steering Angle vs. Yaw Rate Varying Velocity (a), and Aircraft Type (b).**

The MATLAB script was then used to solve for the time response of  $\psi$  and  $\dot{\psi}$  for a step change in steering angle command. A tire relaxation effect was also added by using the time-dependent formula for slip angle provided by [8]. This formula was updated to the current tire coordinate system and is provided below:

$$\sigma \dot{\alpha} = -V_x \tan(\alpha) + V_y \quad (20)$$

The results are shown in Fig. 5 with and without the tire relaxation effect. These results show the tire relaxation effect is more impactful at low speeds, where it alters the character of the yaw rate response, but in general the settling time and final value of the yaw rate response is not impacted. For each response in Fig. 5, a classical first order time delay response is plotted with the time constant calculated through Eq. (16). Note that velocity is provided in m/s and steering angle in degrees for Fig. 5.

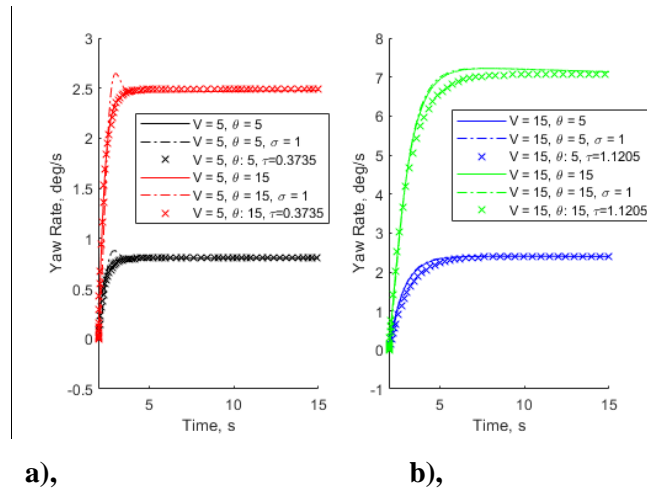


**Fig. 5 Yaw Rate Response to Step Steering Command for Low (a) and High (b) Velocity**

A negative steering delay was implemented into the final steering command vector that causes the aircraft to begin the maneuver slightly before the derived formula would initially specify. The steering delay accounts for the lag between command and aircraft response and can be used to correct the aircraft path.

### C. Thrust and Braking Profile Determination

In this model, the required aircraft thrust is defined by the aircraft mass times the required acceleration defined by the velocity profile. It was assumed that differential thrust is not used for the steering maneuver. Thrust is added to overcome the rolling drag of the tires; the rolling drag is calculated by multiplying  $\mu_R$  by  $F_Z$  as provided in Eqs. (21) and (22).

$$T = m_{AC} * a + \sum_{i=1}^{\#LG} \mu_R F_{Z,i} \quad (21)$$

The thrust profile can be corrected from previous simulation results in an iterative process. For each timestep, the required acceleration is compared to the measured accelerations. Additional thrust is added or subtracted to the last used thrust profile to correct the error between required and measured accelerations.

$$T = T_0 + m_{AC} * \{(a)_{required} - (a)_{last}\} \quad (22)$$

Note that if the required  $a$  is less than zero, a negative thrust may result from this calculation. This can represent either reverse thrust or a braking force. If braking is required, first the thrust profile is determined. Then, the minimum thrust is applied, with any values beneath the minimum thrust assigned to a desired braking force.

The desired braking force is converted to a desired longitudinal friction coefficient by dividing by the vertical force on each MLG tire, which is  $F_{Z,MLG}$ , calculated via Eq. (9), divided by  $N_T$ . The desired longitudinal friction coefficient can be converted to a desired tire slip ratio by dividing by  $K_X$ . The antiskid system functions by multiplying the input  $E$ , a fraction between 0 and 1, by  $s_m$  to obtain an input braking slip ratio, so dividing the desired slip ratio by this value provides the estimated braking command. Finally, tuning factor  $B$  is applied to allow the user control over the amplitude of the resulting braking profile. This relation is summarized below:

$$E = B \left( \frac{1}{s_m} \right) \left( \frac{1}{K_X} \right) \left( \frac{N_T}{F_{Z0}} \right) F_{Brake} \quad (23)$$

## IV. Testing and Verification

To verify the taxi model, a series of simulation test cases using Narrow and Wide-Body Commercial aircraft models (visualized in Fig. 6) with different aircraft paths were performed. The Wide-Body Commercial aircraft has larger length, span, and inertia, in addition to having a four-wheel MLG. Tests were run with an initial steering delay of zero seconds, and then the steering delay was measured from the difference between the taxi model and GearSim in the yaw rate plot. Similarly, the  $A_1/A_2$  values were determined from taking the percent difference in amplitude of the yaw rate plot.

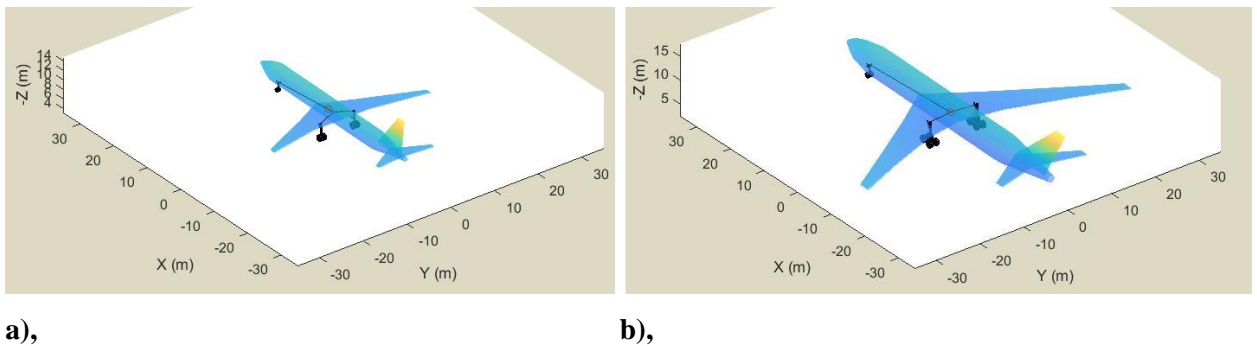
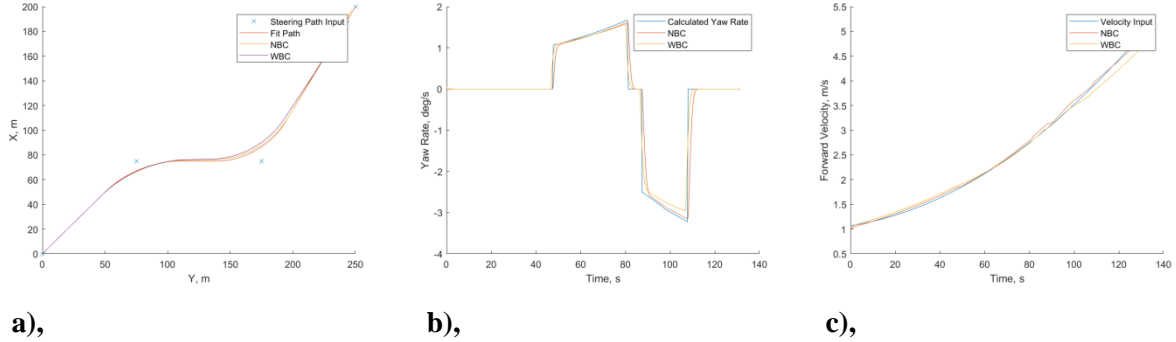


Fig. 6 Visualization of Narrow (a) and Wide-Body Aircraft Models (b).



A cubic curve path was set up, with the aircraft accelerating from 1 to 5 m/s over the course of the maneuver. The steering factor was  $A_1 = A_2 = 1$  and a steering delay of 1 second was applied for the wide body aircraft. The results of this analysis are shown in Fig. 7, and demonstrate that even for the fully nonlinear case of the GearSim simulation; the basic linear relationship in Eq. (19) provides the means to predict the steering command to match a given path.



**Fig. 7 Simulated Aircraft Path (a), Yaw Rates (b), and Forward Velocity (c)**

## V. Conclusion

This paper presents the development of a taxi analysis simulation, provides an outline as to how the algorithm currently operates, and provides an example of the potential for the algorithm to provide a realistic simulation of an aircraft following an arbitrary path. An analysis of aircraft steering provided equations to predict both the steering angle for a given aircraft yaw rate, and the settling time of aircraft yaw rate to a provided steering command. These equations lay a foundation for the taxi algorithm to predict the steering and thrust commands to enable GearSim's aircraft model to follow a predetermined path in a realistic simulation.

The taxi algorithm was designed with a narrow-body commercial aircraft as a primary test case, and is able to provide predictions for the steering, thrust, and braking profiles that match the desired paths for this aircraft with a low error. This method is suitable for use in detailed landing gear modeling and simulation, and has been integrated into SDI's GearSim software and has also been tested on a series of other commercial and military aircraft models with similarly low error. Landing gear and subsystem design engineers can utilize realistic taxi simulations to understand the ground loads and detailed loading conditions for their subsystems in routine taxi maneuvers. For example, many landing gear subsystems are designed for their most critical load case, but for fatigue and tire wear, the detailed loading conditions during routine maneuvers are also required. The developed taxi algorithm could be applied to improve autopilot systems for taxi maneuvers, or provide taxiing aid to a pilot after landing at an unfamiliar airport or in unfavorable weather conditions. This algorithm could also be modified to provide greater safety when taxiing by avoiding off-runway excursions, or potentially reduce landing gear and subsystem loading by optimizing the taxi path.

Future work will develop a PID-based pilot model to further enable realistic simulation of aircraft along specific paths. The numerical time delay predictions of the yaw rate response could also be included in the taxi algorithm, with a more detailed first-order time delay model replacing the negative steering delay used in this paper. The use of differential thrust and braking to assist turns will also be integrated into the taxi module.

## References

- [1] Nagai, M., Shino, M., and Gao, F., "Study on integrated control of active front steer angle and direct yaw moment," *JSAE Review*, Vol. 23, No. 3, 2002, pp. 309-315.  
DOI: [10.1016/S0389-4304\(02\)00189-3](https://doi.org/10.1016/S0389-4304(02)00189-3)
- [2] Matsumoto, N. and Tomizuka, M., "Vehicle lateral velocity and yaw rate control with two independent control inputs," *1990 American Control Conference*, 1990, pp. 1868-1875.  
DOI: [10.23919/ACC.1990.4791052](https://doi.org/10.23919/ACC.1990.4791052)
- [3] Manning, W. J., and Crolla, D. A., "A review of yaw rate and sideslip controllers for passenger vehicles," *Transactions of the Institute of Measurement and Control*, Vol. 29, No. 2, 2007, pp. 117-135.  
DOI: [10.1177/0142331207072989](https://doi.org/10.1177/0142331207072989)
- [4] Georgieva, K., and Serbezov, V., "Mathematical Model of Aircraft Ground Dynamics," *2017 International Conference on Military Technologies (ICMT)*, 2017, pp. 514-519.  
DOI: [10.1109/MILTECHS.2017.7988812](https://doi.org/10.1109/MILTECHS.2017.7988812).
- [5] Rankin, J., Coetzee, E., Krauskopf, B., and Lowenberg, M. "Bifurcation and Stability Analysis of Aircraft Turning on the Ground," *Journal of Guidance, Control, and Dynamics*, Vol. 32 No. 2, 2009, pp. 500-511.  
DOI: [10.2514/1.37763](https://doi.org/10.2514/1.37763)
- [6] Vantsevich, V. V., and Gray, J. P., "Relaxation Length Review and Time Constant Analysis for Agile Tire Dynamics Control," *ASME 2015 International Design Engineering Technical Conferences and Computers and Information In Engineering Conference*, Vol. 57106, American Society of Mechanical Engineers, 2015, pp. V003T01A038.  
DOI: [10.1115/DETC2015-46798](https://doi.org/10.1115/DETC2015-46798)
- [7] Wei, C., and Olatunbosun, O. A., "The effects of tyre material and structure properties on relaxation length using finite element method," *Materials & Design*, Vol. 102, 2016, pp. 14-20.  
DOI: [10.1016/j.matdes.2016.04.014](https://doi.org/10.1016/j.matdes.2016.04.014)
- [8] Besselink, I. J. M., Schmeitz, A. J. C., and Pacejka, H. B., "An improved Magic Formula/Swift tyre model that can handle inflation pressure changes," *Proceedings of the 21st Symposium of the International Association for Vehicle System Dynamics (IAVSD 09)*, edited by In M. Berg, and A. S. Trigell, Vol. 48, Vehicle System Dynamics: International Journal of Vehicle Mechanics and Mobility; No. suppl. 1), 2010, pp. 337-352.  
DOI: [10.1080/00423111003748088](https://doi.org/10.1080/00423111003748088)
- [9] Richards, P. W. and Erickson, A., "Dynamic Ground Loads Analysis Using Detailed Modeling of Landing Gear and Aircraft Aeroservoelastics," *AIAA SciTech 2019 Forum*, San Diego, 2019.  
DOI: [10.2514/6.2019-0759](https://doi.org/10.2514/6.2019-0759)
- [10] McDonald, M., Richards, P. W., Walker, M., and Erickson, A. J., "Carrier Landing Simulation using Detailed Aircraft and Landing," *AIAA SciTech 2020 Forum*, Orlando, 2020.  
DOI: [10.2514/6.2020-1138](https://doi.org/10.2514/6.2020-1138)